

Article

In Vitro Bioaccessibility and Health Risk of Heavy Metals from PM_{2.5}/PM₁₀ in Arid Areas—Hotan City, China

Bowen Liu ^{1,2}, Yuanyu Zhang ^{1,2}, Dilinuer Talifu ^{1,2,*} , Xiang Ding ^{3,4,*} , Xinming Wang ^{3,4} ,
Abulikemu Abulizi ^{1,2}, Qilong Zhao ^{1,2}, Xiaohui Zhang ^{1,2} and Runqi Zhang ³

- ¹ State Key Laboratory of Chemistry and Utilization of Carbon Based Energy Resources, School of Chemical Engineering and Technology, Xinjiang University, Urumqi 830017, China; 995927921@stu.xju.edu.cn (B.L.); zql1998@stu.xju.edu.cn (Q.Z.); xiaohuizhang@stu.xju.edu.cn (X.Z.)
- ² Xinjiang Key Laboratory of Coal Clean Conversion & Chemical Engineering, College of Chemical Engineering, Xinjiang University, Urumqi 830017, China
- ³ State Key Laboratory of Organic Geochemistry, Guangzhou Institute of Geochemistry, Chinese Academy of Sciences, Guangzhou 510640, China
- ⁴ Guangdong-Hong Kong-Macao Joint Laboratory for Environmental Pollution and Control, Guangzhou 510640, China
- * Correspondence: dilnurt@xju.edu.cn (D.T.); xiangd@gig.ac.cn (X.D.)

Abstract: The impact of heavy metals in particulates plays an assignable role in human health—especially in the northwest region of China, which is affected by severe dust storms—and the bioaccessibility and health risks of heavy metals in particulate matter have not yet been quantified and evaluated. This study used Gamble’s solution and PBET (physiologically based extraction test) experiments to simulate the human respiratory and digestive systems, and analyzed the concentrations and bioaccessibility of Pb, Mn, Ni, Cd and As in PM_{2.5} and PM₁₀ samples in the urban area of Hotan City during summer (July) and winter (January). The result shows that Mn and Pb are the most abundant elements in five metals. The bioaccessibility of Mn in gastric fluid was the highest in both summer (PM_{2.5}: 64.1%, PM₁₀: 52.0%) and winter (PM_{2.5}: 88.0%, PM₁₀: 85.1%). Meanwhile, in the respiratory system, the highest bioaccessibility of PM_{2.5} and PM₁₀ in summer was Ni (53.3%), and Pb (47.9%), respectively. Although the concentration of Cd is low in winter, its bioaccessibility in lung fluid was the highest (PM_{2.5}: 74.7%, PM₁₀: 62.3%). The USEPA standard model and Monte Carlo simulation results show that the heavy metals in PM_{2.5} and PM₁₀ would give rise to non-carcinogenic risk for both adults and children through the respiratory system in summer but had little risk in winter. However, the metal may have non-carcinogenic risk to children through intake. In addition, there is a cancer risk to adults through the respiratory system in winter (PM_{2.5}: CR = 1.80 × 10^{−6}, PM₁₀: CR = 2.82 × 10^{−6}), while there is a carcinogenic risk through the digestive system regardless of season and age.

Keywords: PM_{2.5}; PM₁₀; heavy metals; bioaccessibility; Hotan



Citation: Liu, B.; Zhang, Y.; Talifu, D.; Ding, X.; Wang, X.; Abulizi, A.; Zhao, Q.; Zhang, X.; Zhang, R. In Vitro Bioaccessibility and Health Risk of Heavy Metals from PM_{2.5}/PM₁₀ in Arid Areas—Hotan City, China. *Atmosphere* **2023**, *14*, 1066. <https://doi.org/10.3390/atmos14071066>

Academic Editor: Lena Novack

Received: 17 May 2023

Revised: 11 June 2023

Accepted: 21 June 2023

Published: 24 June 2023



Copyright: © 2023 by the authors. Licensee MDPI, Basel, Switzerland. This article is an open access article distributed under the terms and conditions of the Creative Commons Attribution (CC BY) license (<https://creativecommons.org/licenses/by/4.0/>).

1. Introduction

Atmospheric particulate matter (PM) plays an important role in climate change, human health and ecosystems, and is currently the subject of extensive research by relevant scholars around the world [1,2]. Inhalable particulate matter refers to PM with an aerodynamic equivalent diameter less than 10 μm. Due to the PM having complex composition (organic substances, inorganic salts and heavy metals) and an ability to accumulate in the lungs for a long time, they can easily cause asthma, arrhythmia, bronchitis and other diseases, increasing mortality [3–6]. From 1990 to 2019, the number of deaths caused by air pollution worldwide increased by 2.62% [7]. Additionally, more than 90% of the world’s population lives in areas that do not meet the air quality standards set by the WHO [8]. Hence, PM was listed as a Class I pollutant by the International Agency for Research on Cancer (IARC) [9].

PM toxicity is thought to depend on the chemical composition and size of the particles [10]. Toxicological studies show that heavy metals in PM are harmful to human health; transition metals in PM can catalyze the formation of ROS (reactive oxygen species), leading to respiratory inflammation [11,12]; Pb and As will damage the nervous, respiratory and cardiovascular systems and impact physical and intellectual development [13,14]. The latest research shows that exposure to Pb during pregnancy will affect the nervous system, and this exposure is not conducive to fetal development [8]. Heavy metals threaten human health through the respiratory system [15]. Some studies also show that heavy metals will accumulate in food with the sedimentation of particles and enter the human body through ingestion [16–18].

Heavy metals entering the lung through the respiratory system may interact with lung fluid through different mechanisms such as paracellular transport and trans-cellular transport; at this point, diffusion is the main transport mechanism of heavy metals [19]. Additionally, upon intake, heavy metals in the body will cross the gastrointestinal epithelium, reach the central compartment and become available for distribution to internal target tissues and organs [20]. The impact of heavy metals on health depends on their total content, toxicity, bioaccessibility and other factors related to inhalation exposure [21]. Many studies have utilized the total concentration of heavy metals for health risk assessment in recent years [22,23]. However, some study have shown that only the bioaccessible fraction of heavy metal can be absorbed by the human body [24]. Therefore, using total metal concentration will lead to a higher coefficient of risk assessment.

The bioaccessibility test has been developed by the Bioaccessibility Research Group of Europe (BARGE) and is known as the Unified BARGE Method (UBM) [25]. The bioaccessibility of metals indicates the extent and rate of their absorption by biological systems, and its value depends on surface characteristics of the metal, bonding strength and the nature of the solution [26,27]. At present, the bioaccessibility of heavy metals is mainly determined through in vivo (animal experiments) and in vitro experiments. In vivo experiments can obtain more accurate results by analyzing the intestines and excreta of animals, but the operation is complex, time-consuming and expensive [25]. In addition, for in vitro experiments, ultrapure water was generally used as the solvent to explore the bioaccessibility in early times [28,29]; however, the solubility of heavy metals in human body fluid is very different from ultrapure water due to different factors such as the pH of dissolution medium [30,31]. Therefore, people have developed a variety of simulated human body fluids to evaluate the bioaccessibility of heavy metals. Gamble solution and Artificial Lysosomal Fluid (ALF) are widely used in vitro methods and simulate human lung fluid [21,32]; PBET simulates the absorption of heavy metals by the digestive system [33,34]. It has been proved that there is a good correlation between in vitro methods and animal experiments [25,35]. Until now, most studies on bioaccessibility of heavy metals were concentrated in soil, road dust and water samples [32–34]. However, this study focuses on the bioaccessibility of heavy metals in PM.

Hotan is located in the south of Xinjiang, China, close to the Taklimakan Desert. The desert area has an extremely dry climate and frequent sandstorms. Therefore, Hotan has a very high number of floating dust and sandstorm days in summer; this causes a significant increase in PM₁₀ concentration and seriously affects human health. Previous studies had shown that the main sources of Mn and Ni were soil and resuspended dust [36]; vehicle emissions and coal combustion may also raise the concentration of Pb, Cd and As in the air [36,37]. There are a certain number of vehicles and tire maintenance industries in the urban area of Hotan, as well as a large number of residential areas and schools, which may lead to the enrichment of these metals in particulate matter. Previous research on heavy metals in arid areas has spent more attention on concentration and source [38]. Bao et al. analyzed the concentration and health risks of heavy metals in particulate matter in Hotan City in the summer of 2020 [39]. The results showed that Mn and Cr had non-carcinogenic and carcinogenic risks for children and adults, while As only had carcinogenic risks for

adults in dusty weather. However, there are currently no reports on the bioaccessibility of heavy metals in Hotan.

Therefore, in this study, the concentrations of Pb, Mn, Ni, Cd and As in different particle sizes of atmospheric particulates in Hotan City was analyzed, *in vitro* bioaccessibility of heavy metals was detected for the first time in this area and the factors influencing the bioaccessibility of metals were analyzed. Using the above analysis data, the health risks of heavy metals for adults and children were calculated for both winter and summer and the results were optimized using Monte Carlo simulations. The data provide a theoretical basis for pollution control in local and similar regions.

2. Materials and Methods

2.1. Sampling Site Description and Particulate Matter Collection

The sampling site (43°46'29" N, 87°37'18" E) was set on the roof of the ecological environment monitoring station in Hotan (Figure 1). The sampling site was close to the main road of Hotan (about 100 m), nearly 20 m above the ground; the sampling site is surrounded by residential buildings, commercial streets and major traffic roads. Two Laoying-2031 high-flow particulate matter samplers (LaoYing Environmental Technology Co., Ltd, Qingdao, China) were used to simultaneously collect PM_{2.5} and PM₁₀ samples (particle aerodynamic diameters less than 2.5 and 10 µm, respectively) with a sampling flow of 1.05 m³/min. A quartz fiber filter (203 × 254 mm, Whatman, Britain) was used for sampling collection. Sampling was suspended when it rained or snowed and resumed again when the weather improves.

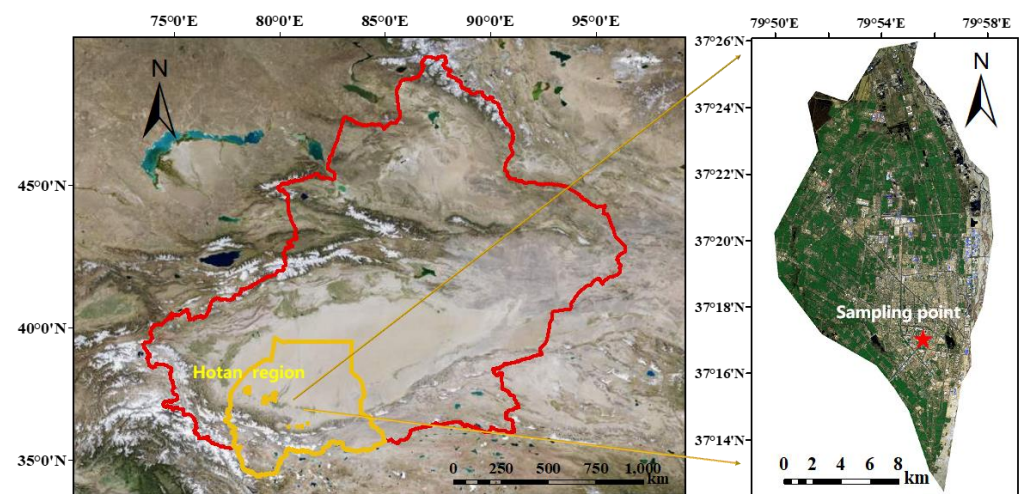


Figure 1. Location of the sampling site.

The sample collection of PM_{2.5} and PM₁₀ during the winter in Hotan was performed from 30 December 2019 to 19 January 2020. The total sampling time was 22 h (from 10:00 am to 8:00 am the next day). The PM_{2.5} and PM₁₀ samples during the summer were obtained from 5 July to 26 July 2020. Frequent dusty weather in summer may oversaturate the sampling film; therefore, each individual sampling day was divided into daytime (from 10:30 to 19:30, 9 h) and nighttime (from 24:00 to 9:00 the next day, also 9 h) sampling in summer. The total daily sampling periods during the summer was 18 h. The day and night samples were analyzed together during the experimental process.

2.2. Quantitative Analysis of Heavy Metals

The samples of PM were cut with a clean filter cutter with a diameter of 2.54 cm (5.06 cm² in area); then, clean Teflon scissors were used to cut it into pieces and place it in a Teflon digestion container. A total of 5 mL 65% HNO₃, 1 mL 30% H₂O₂ and 1 mL 40% HF were added to the container, the digestion container was covered and an electric hot plate (EH20A-plus hot plate, Labtech Company, Hopkinton, MA, USA) was used to raise the

temperature to 210 °C for 5 h until the sample was completely digested. Then, the digestion container was opened and heating continued to evaporate the acid until almost dry. After that, the residual solution was transferred into the colorimetric tube, a small amount of ultrapure water was added into the digestion container many times to dissolve the residual heavy metals and acids and they were transferred to the colorimetric tube. A total of 1 mL 37% HCl was added to provide an acidic environment and the solution volume was made to reach 25 mL with ultrapure water. The concentrations of Pb, Mn, Ni, Cd and As in the solution were quantitatively detected by ICP-AES (Optima8000, PerkinElmer Company, Shelton, CT, USA). The detection limits for each metal are shown in Table S1. The blank control group and samples were analyzed in parallel to reduce the impact of residual metal on the experimental results.

2.3. Bioaccessibility Analysis of Heavy Metals in PM

2.3.1. Simulated Body Fluid Experiment

Gamble solution [40] and PBET [41,42] were used to simulate the interstitial fluid in the lung and gastric fluid and intestinal fluid, respectively. The composition of the two solutions is shown in Table S2.

Simulation of lung fluid experiment: The samples of PM were cut with a filter cutter with a diameter of 4.7 cm (17.35 cm² in area). The remainder of the procedure was as follows. Cut it into pieces and add it into the simulated lung fluid according to the solid–liquid ratio of 1:1000. Shake it for 24 h at 37 °C and 100 rpm (SHA-B water bath thermostatic oscillator, Jintan Medical Instrument Factory, Jiangsu, China). Then, centrifuge for 15 min at 10,000 rpm (H1750 centrifuge, Xiangyi Laboratory Instrument Development Co., Ltd, Hunan, China) and use a syringe filter (0.45 µm) to remove impurities from the supernatant after centrifugation. Finally, the content of Pb, Mn, Ni, Cd and As in solution was analyzed by ICP-AES (Optima8000 inductively coupled plasma emission spectroscopy).

Simulation of gastric fluid experiment: PM_{2.5} and PM₁₀ samples were cut with a 2.54 cm diameter (5.06 cm²) filter cutter precisely. The samples were added to a simulated gastric solution in a 1:100 solid–liquid ratio at 37 °C and shaken at 100 rpm for 1 h. The samples were then centrifuged at 10,000 rpm for 15 min and filtered through a syringe filter (0.45 µm). After that, they were analyzed by ICP-AES for the content of Pb, Mn, Ni, Cd and As in solution.

Simulation of intestinal fluid experiment: The pH of the solution was adjusted to 7 with saturated NaHCO₃ solution after the simulated gastric phase and trypsin (0.05 g) and bile salts (0.175 g) were added into the reaction solution of gastric juice. The solution was shaken in a water bath at 37 °C and 100 rpm for 4 h. During the shaking process, the pH value of the solution was measured every 15 min and maintained at 7 by dropping 12 mol/L of HCl or saturated NaHCO₃ solution. After shaking, the solution was centrifuged at 10,000 rpm for 15 min and filtered through a syringe filter (0.45 µm). Then, quantitative analysis by ICP-AES was performed.

2.3.2. Calculation of Bioaccessibility of Heavy Metals

The bioaccessibility of heavy metals in PM in different simulated environments of the human body is calculated by the following equation [43]:

$$BA_i = \frac{C_{SIMi} \times V_{SIM}}{C_i \times M_T} \times 100\% \quad (1)$$

where BA_i is the bioaccessibility of heavy metal in the simulated liquid of PM (%); C_{SIMi} is the concentration of heavy metal in the simulated solution in vitro (µg/mL); V_{SIM} is the volume of simulated solution in each reactor (mL); C_i is the content of metal in the sample (µg/g); and M_T is the mass (g) of the PM sample added to the simulated liquid.

2.4. Human Health Risk Assessment

2.4.1. Exposure Assessment

The health risks of heavy metals in PM_{2.5} and PM₁₀ in Hotan urban area were estimated according to the human health evaluation manual (Part A) and the supplementary guidance for inhalation risk assessment (Part F) [44]. The model evaluates the exposure values of adults and children in the respiratory and digestive systems in terms of the chemical daily intake (CDI) and exposure concentration (EC) (relevant parameters and calculation results can be found in Tables S3–S6). The equation as follows:

$$EC_{inh} = \frac{C \times BA \times EF \times ED \times ET}{AT_h} \quad (2)$$

$$CDI_{ing} = \frac{C \times BA \times IngR \times EF \times ED}{BW \times AT_d} \times CF \quad (3)$$

where C is the total concentration of metals in PM_{2.5} and PM₁₀ ($\mu\text{g}/\text{m}^3$ for inhalation exposure, mg/kg for intake exposure); BA is the bioaccessibility of metals in simulated solution (%); ET is exposure time (24 h/day); AT_h is the average time (for carcinogen: $AT_h = 70 \text{ years} \times 365 \text{ days} \times 24 \text{ h}$; for non-carcinogens: $AT_h = ED \times 365 \text{ days} \times 24 \text{ h}$); $IngR$ represent the ingestion rate (the value provided by the USEPA for soil dust risk assessment was utilized in this study); BW is the average body weight (kg); EF is exposure rate (day/year); ED is the exposure duration (year); AT_d is averaging time (for carcinogens, $AT_d = 70 \text{ years} \times 365 \text{ days}$; for non-carcinogenic, $AT_d = ED \times 365 \text{ days}$); and CF is the conversion factor ($10^{-6} \text{ kg}/\text{mg}$).

2.4.2. Risk Assessment

According to the calculation model of the USEPA [44], the hazard quotient (HQ) and hazard index (HI) are used to assess the non-carcinogenic risk. HI is the sum of HQ for each metal. If the values of HQ and HI are less than 1, the non-carcinogenic risk is almost non-existent; if the value of HQ and HI are greater than 1, it means that there may be a risk of carcinogenicity, and the greater the value of HQ and HI, the higher the non-carcinogenic risk. The non-carcinogenic risk of inhalation (HQ_{inh}) and intake (HQ_{ing}) is calculated by the following equations.

$$HQ_{inh} = \frac{EC_{inh}}{RfCi \times 1000 \mu\text{g}/\text{mg}} \quad (4)$$

$$HQ_{ing} = \frac{CDI_{ing}}{RfDo} \quad (5)$$

$$HI = \sum HQ_i \quad (6)$$

where $RfDo$ is the oral reference dose ($\text{mg}/\text{kg} \text{ day}$) and $RfCi$ is the inhalation reference concentration (mg/m^3).

CR is the carcinogenic risk of pollutants, which usually represents the probability of cancer, and is expressed by the number of cancer patients in a specific population. For example, if CR is between 10^{-6} – 10^{-4} (i.e., 1 additional patient per 10,000 to 1,000,000 people), the substance is considered to have a potential carcinogenic risk. If the CR value is less than 10^{-6} , it means there is almost no carcinogenic risk. In the following equation, the carcinogenic risks of inhalation and ingestion are calculated by (CR_{inh}) and (CR_{ing}), respectively.

$$CR_{inh} = IUR \times EC_{inh} \quad (7)$$

$$CR_{ing} = CDI_{ing} \times SFo \quad (8)$$

where IUR is the inhalation unit risk ($(\mu\text{g}/\text{m}^3)^{-1}$) and SFo is the oral slope factor ($(\text{mg}/\text{kg} \text{ day})^{-1}$).

2.5. Quality Control and Quality Assurance

The setting of sampling sites and the number of samples meet the requirements of Technical Specifications for the Layout of Ambient Air Quality Monitoring Points (HJ 664—2013) (http://www.mee.gov.cn/ywgz/fgbz/bz/bzwb/jcffbz/201309/t20130925_260810.shtml. Accessed on 1 September 2019.) and Ambient Air Quality Standard (GB 30952012) (http://www.mee.gov.cn/ywgz/fgbz/bz/bzwb/dqhjbh/dqhjzlbz/201203/t20120302_224165.shtml. Accessed on 1 September 2019.). The sampling process is strictly in accordance with the standards specified in the Technical Specifications for the Layout of Ambient Air Quality Monitoring Points (HJ 664-2013) and the Technical Specifications for Manual Monitoring Method (Gravimetric Method) of Ambient Air Particulate Matter (PM_{2.5}) (HJ 656-2013) (http://www.mee.gov.cn/ywgz/fgbz/bz/bzwb/jcffbz/201308/t20130802_256857.shtml. Accessed on 1 September 2019.).

Blank samples were collected for 10 min (the sampler was not turned on), and the steps for collecting blank samples were the same as those for particulate matter samples. The sampling films were stored at low temperature to avoid contamination. Weighing was fully balanced to ensure constant humidity and temperature. The average value was taken by weighing three times and the error of each weighing result was controlled within 0.05 mg. Blank control groups were collected at each sampling. The experimental analysis process of blank samples was consistent with the particulate matter samples, and the Coefficient of Variation (COV) of the result is shown in Table S9.

3. Results and Discussion

3.1. Distribution of Heavy Metals in PM_{2.5} and PM₁₀ in Different Sampling Periods

The concentrations of PM_{2.5} and PM₁₀ in the Hotan urban area were $129.8 \pm 40.5 \mu\text{g}/\text{m}^3$ and $155.2 \pm 44.8 \mu\text{g}/\text{m}^3$ in winter and $205.6 \pm 108 \mu\text{g}/\text{m}^3$ and $361.3 \pm 232.6 \mu\text{g}/\text{m}^3$ in summer (Table 1). The total average mass concentrations of five heavy metals in PM_{2.5} and PM₁₀ in winter were 96.58 ± 21.05 and $166.11 \pm 44.03 \text{ ng}/\text{m}^3$, respectively; Pb had the highest concentration of particles of different particle sizes (PM_{2.5}: $51.69 \text{ ng}/\text{m}^3$, PM₁₀: $76.88 \text{ ng}/\text{m}^3$). In summer, the average concentrations of five heavy metals in PM_{2.5} and PM₁₀ were 90.78 ± 93.50 and $257.98 \pm 89.26 \text{ ng}/\text{m}^3$, respectively; the main metal in the particulate matter was Mn (PM_{2.5}: $70.17 \text{ ng}/\text{m}^3$, PM₁₀: $122.63 \text{ ng}/\text{m}^3$). The above data shows that the average concentration of heavy metals in PM₁₀ in summer is higher than that in winter. Previous studies have shown that the mass concentrations of metal elements (crustal and anthropogenic elements) in PM_{2.5} in the urban areas of Hotan in 2014 were twice as high in summer as in winter, and that Cr, Mn, Zn and As were more affected, with their mass concentrations rising by 10–50% in summer compared to winter [45].

Heavy metal concentrations in PM_{2.5} as a percentage of heavy metal concentrations in PM₁₀ are mainly higher in winter than in summer. The proportion of Pb is nearly twice as high in winter (72%) as in summer (38%), while that of Ni (82%, 15%), Cd (66%, 3%) and As (72%, 8%) are 5.5, 22 and 9 times higher in winter than in summer, respectively. The ratio of Mn is basically the same (44%, 48%). One reason for this may be the high level of dusty weather in summer [46]; the content of PM₁₀ in the air increases significantly with the sand and dust, causing a higher ratio of PM_{2.5} to PM₁₀ concentrations in winter than in summer (winter: 0.84, summer: 0.57), resulting in most particles distributed in PM_{2.5} in winter. On the other hand, PM_{2.5} has smaller particle size and larger specific surface area; the wind speed in Hotan City is smaller and the humidity is higher in winter [47]. Low temperatures inhibit the diffusion of pollutants and make it easier for heavy metals to bind to PM_{2.5} [48]. Additionally, Pb, Ni, Cd and As were all associated with coal combustion emissions [36,37,49]; higher winter demand for coal combustion increases its concentration in particulate matter. Mn is mainly from soil [36], and the impact of local anthropogenic emissions is not significant; therefore its change is not obvious.

Table 1. Total concentration (ng/m³) of heavy metals in PM₁₀ and PM_{2.5} and equivalent concentration of metals dissolved in simulated fluid.

		Pb	Mn	Ni	Cd	As
Winter PM ₁₀ = 155.175 ± 44.801 µg/m ³						
Total	Mean ± SD	76.88 ± 14.96	73.39 ± 27.25	6.00 ± 0.78	3.52 ± 0.55	6.32 ± 0.49
Lung fluid extraction	Mean ± SD	31.06 ± 6.04	27.37 ± 10.16	0.97 ± 0.13	2.19 ± 0.34	2.81 ± 0.22
Gastric fluid extraction	Mean ± SD	39.13 ± 7.62	62.46 ± 23.19	2.54 ± 0.33	1.75 ± 0.27	1.07 ± 0.08
Intestinal fluid extraction	Mean ± SD	10.15 ± 1.97	33.98 ± 12.61	1.06 ± 0.14	1.02 ± 0.16	N/A ^a
Winter PM _{2.5} = 129.809 ± 40.488 µg/m ³						
Total	Mean ± SD	51.69 ± 6.01	32.1 ± 12.79	6.17 ± 1.44	1.86 ± 0.24	4.76 ± 0.57
Lung fluid extraction	Mean ± SD	15.90 ± 4.11	13.27 ± 6.20	1.47 ± 0.49	1.32 ± 0.35	1.67 ± 0.43
Gastric fluid extraction	Mean ± SD	33.52 ± 8.66	26.9 ± 12.58	0.69 ± 0.23	0.98 ± 0.26	0.90 ± 0.23
Intestinal fluid extraction	Mean ± SD	7.63 ± 1.97	15.07 ± 7.05	0.68 ± 0.22	0.66 ± 0.18	N/A
Summer PM ₁₀ = 361.277 ± 232.644 µg/m ³						
Total	Mean ± SD	34.08 ± 9.19	122.63 ± 69.01	43.38 ± 10.02	32.44 ± 0.52	25.45 ± 0.52
Lung fluid extraction	Mean ± SD	16.29 ± 4.39	54.45 ± 30.64	14.71 ± 3.40	N/A	N/A
Gastric fluid extraction	Mean ± SD	12.54 ± 3.38	63.77 ± 35.89	4.90 ± 1.13	N/A	N/A
Intestinal fluid extraction	Mean ± SD	13.12 ± 3.54	50.77 ± 28.57	6.07 ± 1.40	N/A	N/A
Summer PM _{2.5} = 205.647 ± 108.045 µg/m ³						
Total	Mean ± SD	11.14 ± 5.15	70.17 ± 80.17	5.25 ± 3.07	1.15 ± 1.36	3.07 ± 3.75
Lung fluid extraction	Mean ± SD	5.36 ± 2.92	35.01 ± 40.01	2.80 ± 1.64	N/A	N/A
Gastric fluid extraction	Mean ± SD	7.23 ± 3.94	44.98 ± 51.39	2.22 ± 1.30	N/A	N/A
Intestinal fluid extraction	Mean ± SD	4.00 ± 2.18	28.14 ± 32.15	1.58 ± 0.92	N/A	N/A

^a: N/A indicates that the concentration is lower than the detection limit.

Previous studies have shown that coal combustion is a major source of Ni in China's urban atmosphere [49], Cd is mainly related to coal emission and steel smelting [37,50] and As is related not only to coal emissions [37] but also to open burning of domestic waste [51]. Table S7 shows the correlation matrix between metal concentrations in PM₁₀ and PM_{2.5} in summer and winter. The results indicate a strong correlation between Ni, Cd and As ($p < 0.01$), from which it can be inferred that Ni, Cd and As may come from the same source. In addition, the concentration of Ni, Cd and As in PM₁₀ samples in summer is much higher than that in winter, while the concentrations in PM_{2.5} do not differ much from those in winter, probably brought about by the long-distance transport of wind and sand in the urban areas of Hotan in summer which has little relationship with local human activities. The average concentration of the Pb element in PM₁₀ and PM_{2.5} in winter was 2.3 and 4.7 times of that in summer, which may be caused by a large number of villages, residential areas and schools distributed near the sampling point, and a large amount of coal burning during winter heating [52,53]. Mn concentrations in both PM₁₀ and PM_{2.5} are higher in summer than in winter, which is different from studies in other urban areas in China [48,54]. Mn is a marker of soil and resuspended dust [36], and there is more sand and dusty weather in Hotan City in summer; the dust carried by strong winds is the main reason for the high content of Mn in PM in summer. The concentration of heavy metals detected in this study has decreased compared with the previous research [45]; this is closely related to the gradual prohibition of coal-fired boilers, the active promotion of transitioning from coal to electricity and other air pollutant control work in recent years.

3.2. Bioaccessibility of Heavy Metals

Table 1 shows that Cd and As were not detected in two particle size segments of the three simulated solutions in summer. The concentration of Pb in lung fluid of two particle size segments was the highest in winter (PM₁₀: 31.06 ± 6.04 ng/m³, PM_{2.5}: 16.03 ± 3.6 ng/m³), while that of Mn was the highest in summer (PM₁₀: 54.45 ± 30.64 ng/m³, PM_{2.5}: 35.01 ± 40.01 ng/m³). In simulated gastric fluid and intestinal fluid, Mn showed a higher extraction rate both in seasonal and particle size distribution. The high concentration of metals does not directly indicate that the bioaccessibility of metals is high, which

is related to the form of metals present in the particulate matter and the acidity of the extraction solution, among other factors.

Figure 2 and Table S8 show the bioaccessibility of five heavy metals in three simulated solutions in different seasons and particle sizes. In summer, Pb (69.2%) and Mn (64.1%) in PM_{2.5} showed high bioaccessibility in gastric fluid and Ni (53.3%) in lung fluid. The bioaccessibility of Pb (47.8%) and Ni (33.9%) in PM₁₀ in lung fluid was higher than that in other simulated fluids. In winter, Pb (68.1%) and Mn (88.0%) in PM_{2.5} also showed high bioaccessibility in gastric fluid, while Ni (25%), Cd (74.7%) and As (36.8%) showed high bioaccessibility in lung fluid. All five metals show low bioaccessibility in the intestinal fluid at different particle sizes and seasons. The bioaccessibility of Pb, Mn and Ni in simulated lung fluids was higher in summer than in winter in both particle size, but Cd and As are opposite. Although metal concentrations in PM₁₀ are higher than in PM_{2.5}, the bioaccessibility of metals in PM_{2.5} is generally higher than in PM₁₀ in the same simulated fluid during the same season, except for Pb and As extracted with lung fluid and Ni extracted with gastric fluid for winter samples. It is possible that the high bioaccessibility of PM_{2.5} is due to its large specific surface area, and the risk to human health also increases accordingly. Previous studies have come to similar conclusions [50].

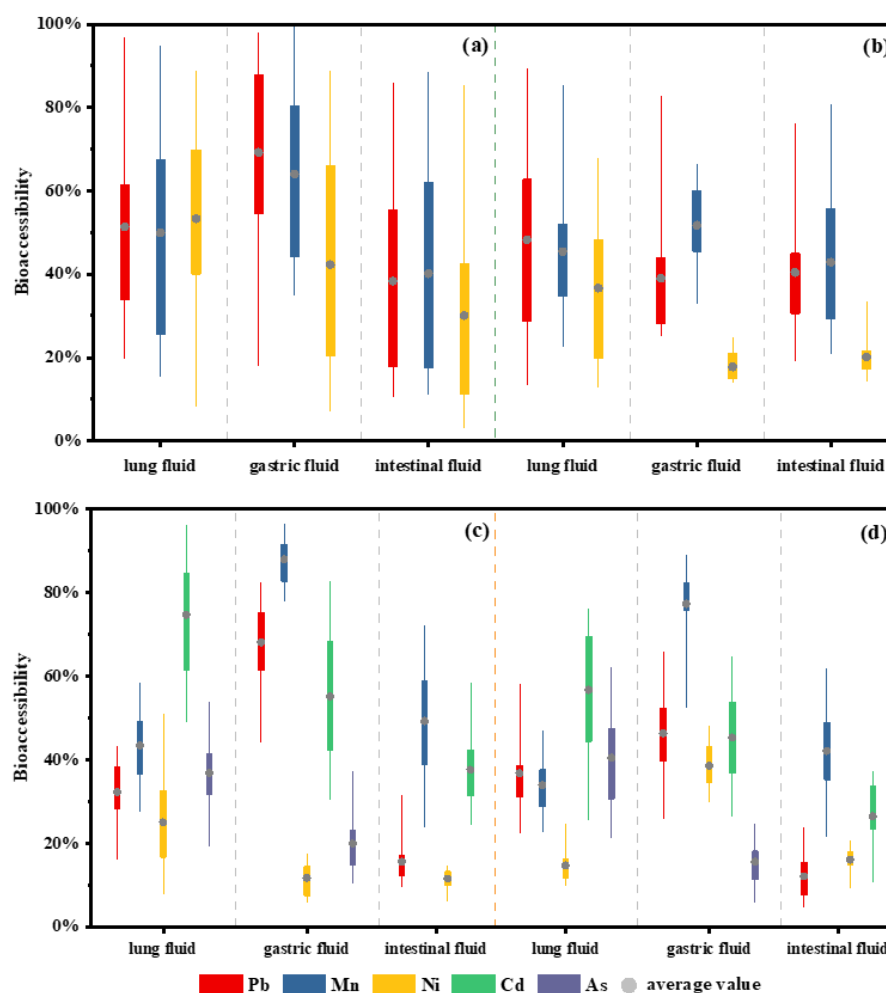


Figure 2. Bioaccessibility of heavy metals in summer (a) PM_{2.5}, (b) PM₁₀ and winter (c) PM_{2.5}, (d) PM₁₀.

Compared with gastric fluid, the bioaccessibility of Pb in lung and intestinal fluid is relatively low. The probable cause is a decrease in the solubility of Pb due to the formation of lead phosphate precipitates with phosphate in the lung fluid [55]. In addition, the pH value of gastric fluid is low, and the stronger acidity leads to increased solubility of Pb [12]; this is

similar to previous studies [34]. Zia et al. suggest that metals bind to protein surface sites, thus forming precipitated material that reduces metal solubility [42]. Simulated lung and intestinal fluid have similar pH, but proteases in the intestinal fluid are negatively charged and provide binding sites that may combine with Pb to form precipitates, resulting in lower Pb concentrations in the intestinal fluid. Sun et al. found that Mn has a large proportion of soluble parts in particulate matter [49], and this is similar to our research results. Mn in particles is mostly combined with oxides, and a lower pH value will significantly increase its solubility in simulated solution, which is similar to the previous research [56]. The bioaccessibility of Mn in summer is much lower than that in winter and has little change in three simulation fluids. The possible reason is that Mn is mainly from soil and suspended dust [36]; sandstorms in summer increase the proportion of oxidizable and residual Mn in the particulate matter, leading to a decrease in its solubility.

For Cd, Ni and other elements that may have cancer risk [21], although the concentration of Cd and Ni in particulate matter is low, its bioaccessibility in simulated fluids cannot be ignored, which is similar to the research results of Saliou et al. [57]. This suggests that Cd and Ni are more readily soluble by human lung and gastrointestinal fluids, which in turn can cause damage to human health. The overall bioaccessibility of As detected in winter was low (less than 20%). Research shows that, although the common form of arsenic (oxygenated anions) is soluble, the solubility of As may be greatly reduced due to the adsorption of amorphous oxides of aluminum and iron, thereby reducing its bioaccessibility [57].

3.3. Health Risk Assessment of Heavy Metals in $PM_{2.5}$ and PM_{10}

The bioaccessibility of metals is only an *in vitro* experiment that explores the extent of extraction of metals in human simulated fluids. However, the Health Risk Assessment (HRA) has been developed to quantitatively evaluate the extent to which environmental pollutants are hazardous to human health. This evaluation system can be calculated by combining the source and concentration of the contaminant, the channel of entry into the human body, the frequency of exposure and human parameters. In this experiment, the exposure values of adults and children in the ingestion and respiration systems were assessed using concentrations of metals in simulated lung and gastric fluids (see Tables S3–S6 for relevant parameters and calculation results), and the non-carcinogenic and carcinogenic risks of adults and children in both systems were assessed using HQ, HI and CR values.

Table 2 shows the carcinogenic and non-carcinogenic risks of Pb, Mn, Ni, Cd and As in $PM_{2.5}$ and PM_{10} in winter and summer in Hotan City through different systems. The HQ for Mn and Cd in PM by the respiratory systems were both higher in winter, and the HQ for Mn and Cd in $PM_{2.5}$ by the respiratory system was 1.37×10^{-1} and 6.85×10^{-2} , respectively. The sum of Mn and Cd contributed 64.6% to the total non-carcinogenic risk value of $PM_{2.5}$. The HQ values in PM_{10} were 2.7×10^{-1} and 1.08×10^{-1} , respectively, accounting for 74.9% of the total non-carcinogenic risk. The HQ values of heavy metals in $PM_{2.5}$ and PM_{10} were higher in Pb and Cd, and the HQ values of Pb and Cd in children (adults) in $PM_{2.5}$ were 5.47×10^{-1} (6.96×10^{-2}) and 5.5×10^{-1} (6.99×10^{-2}), and 4.01×10^{-1} (5.1×10^{-2}) and 6.48×10^{-1} (8.24×10^{-2}) in PM_{10} , respectively. In winter, the risk of ingestion is slightly higher for children than for breathing, while adults show the opposite risk. Additionally, the HQ values for children are higher than for adults in the ingestion system, indicating that heavy metals are more harmful to children at the ingestion stage. Comparison of risk indices also revealed that the risk values for metals were higher for children than for adults. For different particle size segments, the HI value of PM_{10} in the respiratory system is higher than that of $PM_{2.5}$, and the ingestion-stage $PM_{2.5}$ has a higher HI value. On the whole, there is no non-carcinogenic risk ($HQ < 1$) for adults and children in winter through the respiratory system, and the non-carcinogenic risk for adults through the ingestion pathway is also acceptable. However, for children, the HI values for metals in different particle sizes were above the safety limit ($HI = 1$), indicating a non-carcinogenic risk to children from ingestion, and $PM_{2.5}$ was higher than PM_{10} .

Table 2. Non-carcinogenic and carcinogenic health risks for each heavy metal by different pathways in summer and winter (mg/(kg d)).

Toxic Elements		Winter				Summer			
		Hazard Quotient (HQ)		Carcinogenic Risk (CR)		Hazard Quotient (HQ)		Carcinogenic Risk (CR)	
		Children	Adults	Children	Adults	Children	Adults	Children	Adults
		Inhalation pathway							
PM _{2.5}	Pb	— ^a	—	8.48×10^{-9}	3.39×10^{-8}	—	—	2.90×10^{-9}	1.16×10^{-8}
	Mn	1.37×10^{-1}	1.37×10^{-1}	—	—	3.45×10^{-1}	3.45×10^{-1}	—	—
	Ni	5.43×10^{-2}	5.43×10^{-2}	1.56×10^{-8}	6.25×10^{-8}	9.86×10^{-2}	9.86×10^{-2}	2.84×10^{-8}	1.14×10^{-7}
	Cd	6.85×10^{-2}	6.85×10^{-2}	1.06×10^{-7}	4.22×10^{-7}	—	—	—	—
	As	5.77×10^{-2}	5.77×10^{-2}	3.19×10^{-7}	1.28×10^{-6}	—	—	—	—
	Total	3.18×10^{-1}	3.18×10^{-1}	4.49×10^{-7}	1.80×10^{-6}	4.44×10^{-1}	4.44×10^{-1}	3.13×10^{-8}	1.25×10^{-7}
PM ₁₀	Pb	—	—	1.57×10^{-8}	6.30×10^{-8}	—	—	8.27×10^{-9}	3.31×10^{-8}
	Mn	2.70×10^{-1}	2.70×10^{-1}	—	—	5.37×10^{-1}	5.37×10^{-1}	—	—
	Ni	3.42×10^{-2}	3.42×10^{-2}	9.86×10^{-9}	3.94×10^{-8}	5.18×10^{-1}	5.18×10^{-1}	1.49×10^{-7}	5.97×10^{-7}
	Cd	1.08×10^{-1}	1.08×10^{-1}	1.67×10^{-7}	6.68×10^{-7}	—	—	—	—
	As	9.26×10^{-2}	9.26×10^{-2}	5.12×10^{-7}	2.05×10^{-6}	—	—	—	—
	Total	5.05×10^{-1}	5.05×10^{-1}	7.04×10^{-7}	2.82×10^{-6}	1.06×10^0	1.06×10^0	1.58×10^{-7}	6.30×10^{-7}
		Ingestion pathway							
PM _{2.5}	Pb	5.47×10^{-1}	6.96×10^{-2}	1.40×10^{-6}	7.10×10^{-7}	6.45×10^{-2}	8.20×10^{-3}	1.65×10^{-7}	8.37×10^{-8}
	Mn	1.01×10^{-2}	1.29×10^{-3}	—	—	5.30×10^{-3}	6.74×10^{-4}	—	—
	Ni	3.50×10^{-3}	4.46×10^{-4}	5.62×10^{-6}	2.86×10^{-6}	5.40×10^{-3}	6.87×10^{-4}	8.66×10^{-6}	4.40×10^{-6}
	Cd	5.50×10^{-1}	6.99×10^{-2}	—	—	—	—	—	—
	As	1.73×10^{-1}	2.20×10^{-2}	6.69×10^{-6}	3.40×10^{-6}	—	—	—	—
	Total	1.28×10^0	1.63×10^{-1}	1.37×10^{-5}	6.97×10^{-6}	7.52×10^{-2}	9.57×10^{-3}	8.82×10^{-6}	4.49×10^{-6}
PM ₁₀	Pb	4.01×10^{-1}	5.10×10^{-2}	1.02×10^{-6}	5.20×10^{-7}	8.74×10^{-2}	1.11×10^{-2}	2.23×10^{-7}	1.13×10^{-7}
	Mn	1.50×10^{-2}	1.90×10^{-3}	—	—	8.30×10^{-3}	1.06×10^{-3}	—	—
	Ni	8.27×10^{-3}	1.05×10^{-3}	1.33×10^{-5}	6.74×10^{-6}	1.06×10^{-2}	1.35×10^{-3}	1.70×10^{-5}	8.66×10^{-6}
	Cd	6.48×10^{-1}	8.24×10^{-2}	—	—	—	—	—	—
	As	1.31×10^{-1}	1.67×10^{-2}	5.07×10^{-6}	2.58×10^{-6}	—	—	—	—
	Total	1.20×10^0	1.53×10^{-1}	1.93×10^{-5}	9.84×10^{-6}	1.06×10^{-1}	1.35×10^{-2}	1.72×10^{-5}	8.77×10^{-6}

^a: Since the RfC_i value of Pb and SFo value of Cd are not found, and the carcinogenicity of Mn element is low and no relevant carcinogenic risk coefficient is found, it is expressed in —.

The highest carcinogenic risk value under the respiratory route in winter was As, which was lower in children ($PM_{2.5}$: 3.19×10^{-7} , PM_{10} : 5.12×10^{-7}) than in adults ($PM_{2.5}$: 1.28×10^{-6} , PM_{10} : 2.05×10^{-6}), and the total carcinogenic risk value for metals in PM_{10} was higher than in $PM_{2.5}$. Overall, only adults had a carcinogenic risk under the respiratory route ($CR > 10^{-6}$), and As was the main donation. The winter ingestion stage is similar to the respiratory system, with As in $PM_{2.5}$ remaining the element with the highest carcinogenic risk, showing a higher risk in children (6.69×10^{-6}) than in adults (3.4×10^{-6}), while Ni in PM_{10} has the highest carcinogenic risk with a CR (children: 1.33×10^{-5} , adults: 6.74×10^{-6}) exceeding the safety limit ($CR = 10^{-6}$).

In summer, only Mn, Ni and Zn were evaluated for non-carcinogenic risk because the concentrations of Cd and As were below the detection limit. Similar to the winter results, the overall non-carcinogenic risk is greater by the respiratory system than at the ingestion stage; the highest non-carcinogenic risk under the respiratory system was for Mn, with HQ values of 3.45×10^{-1} and 5.37×10^{-1} in $PM_{2.5}$ and PM_{10} , respectively. The non-carcinogenic risk at the ingestion stage remains higher in children. The comparison results of different particle sizes showed that the non-carcinogenic risk value of PM_{10} was higher than that of $PM_{2.5}$, which was consistent with the results in winter. As a whole, only PM_{10} in the particulate matter in summer can cause non-carcinogenic risk to adults and children through the respiratory system, and the risk by the ingestion pathway is lower than the risk threshold ($HQ = 1$).

Ni is the element with the highest carcinogenic risk in summer, with the respiratory route being lower in children ($PM_{2.5}$: 2.84×10^{-8} , PM_{10} : 1.49×10^{-7}) than in adults ($PM_{2.5}$: 1.14×10^{-7} , PM_{10} : 5.97×10^{-7}) and the ingestion route being higher in children ($PM_{2.5}$: 8.66×10^{-6} , PM_{10} : 1.70×10^{-5}) than adults ($PM_{2.5}$: 4.4×10^{-6} , PM_{10} : 8.66×10^{-6}). The carcinogenic risk of Ni is 1–2 orders of magnitude higher than that of Pb. In general, the distribution pattern is the same as in winter, and the carcinogenic risk for all elements in the respiratory system were less than 10^{-6} , indicating that there is no carcinogenic risk, while in the ingestion route Ni in both PM_{10} and $PM_{2.5}$ poses a carcinogenic risk, and the risk is higher for children.

The disadvantage of using USEPA's standard equation calculations is that only a single result can be calculated, but the variables are uncertain in the actual process, whereas Monte Carlo simulations are often used to deal with risk-related uncertainties by modelling the probability distributions of variables and accumulating a large number of simulations so that the results obtained are closer to the actual situation [58,59]. In conjunction with the equations in this study, the Crystal Ball 11.1 software was used to create probabilistic models for the CR and HI of the five heavy metals analyzed in this research. Some studies have shown that 5000 iterations are sufficient to ensure the stability of the results, with 10,000 simulations giving even more accurate results [60]; the confidence level P was determined as 95%.

Overall, the Monte Carlo simulation results were all nearly an order of magnitude higher than those calculated by the USEPA standard model, and the trends were consistent with those calculated by the USEPA model. In winter (Figure 3) there was little non-carcinogenic risk for adults by the respiratory and ingestion routes, while non-carcinogenic risk was present for children ($HI > 1$ at $P = 95\%$) with higher risk from ingestion. Winter simulations showed that carcinogenic risks existed for both adults and children ($CR > 10^{-6}$ at $P = 95\%$) for all routes, and the ingestion route was an order of magnitude higher than the respiratory route overall. When comparing adults and children, the carcinogenic risk is higher for adults in the respiratory system, and for children, the risk is higher by ingestion route than in adults. Because children and adults have different behaviors every day, some of the children's bad habits, such as frequently putting their hands in their mouths, led to an increased risk of ingestion, which is consistent with the research of Nie et al. [61].

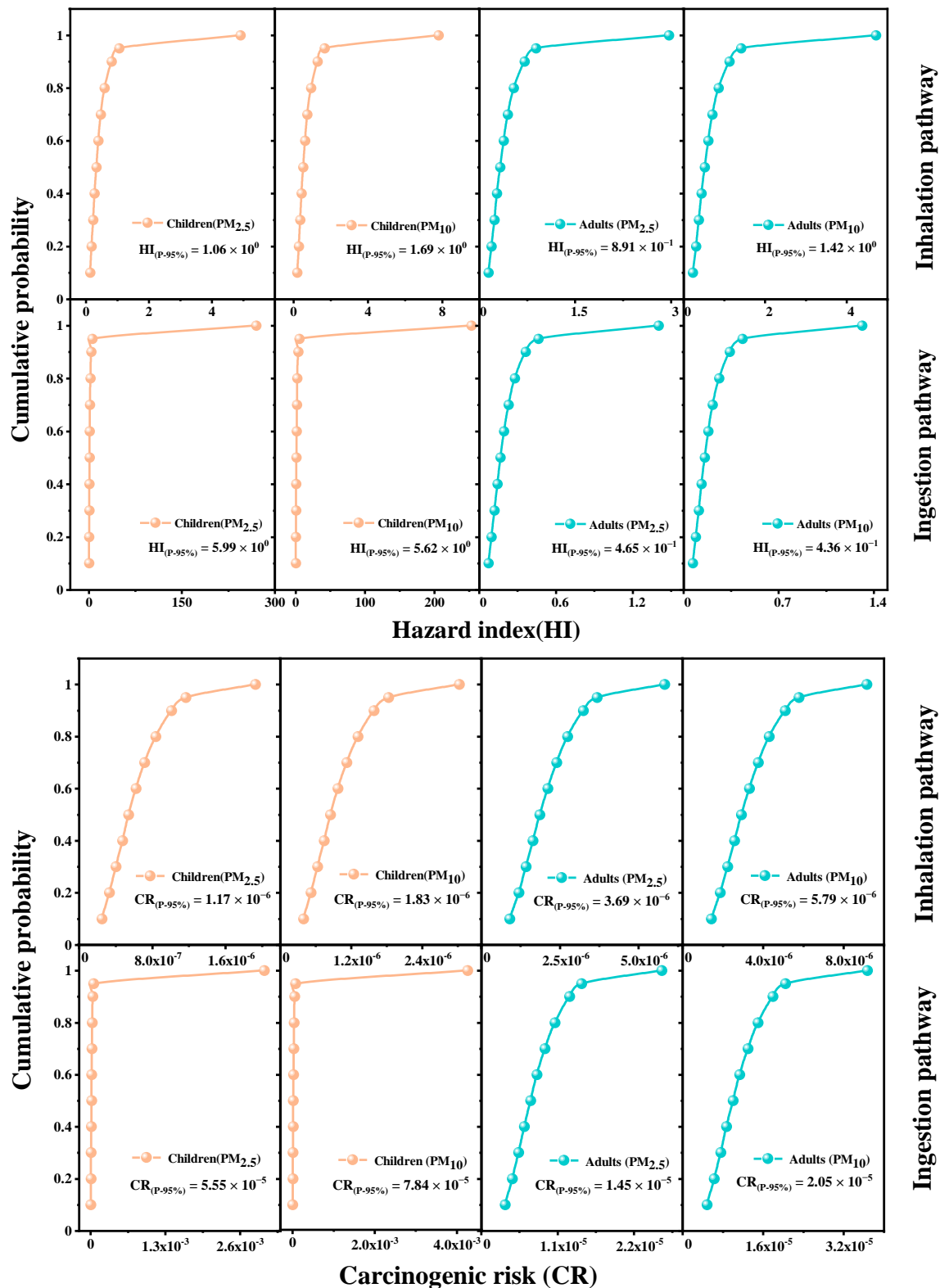


Figure 3. Cumulative probability distribution of carcinogenesis and non-carcinogenesis in winter.

In summer (Figure 4) there is no non-carcinogenic risk for both adults and children by the ingestion route ($P = 95\%$ $HI < 1$), but the non-carcinogenic risk of respiratory system is similar to that of winter, with higher risk for children than for adults. For carcinogenic risk, there is no risk from the respiratory system except for PM₁₀ in adults, but heavy metals can cause carcinogenic risk in all groups of people through the ingestion route, with a greater

impact on children. The effects of heavy metals on adults and children were similar in summer as in winter; it is shown that the risk of carcinogenesis is not correlated with the season, the type and content of metals and the differences in behavior between adults and children are the main factors in carcinogenic risk.

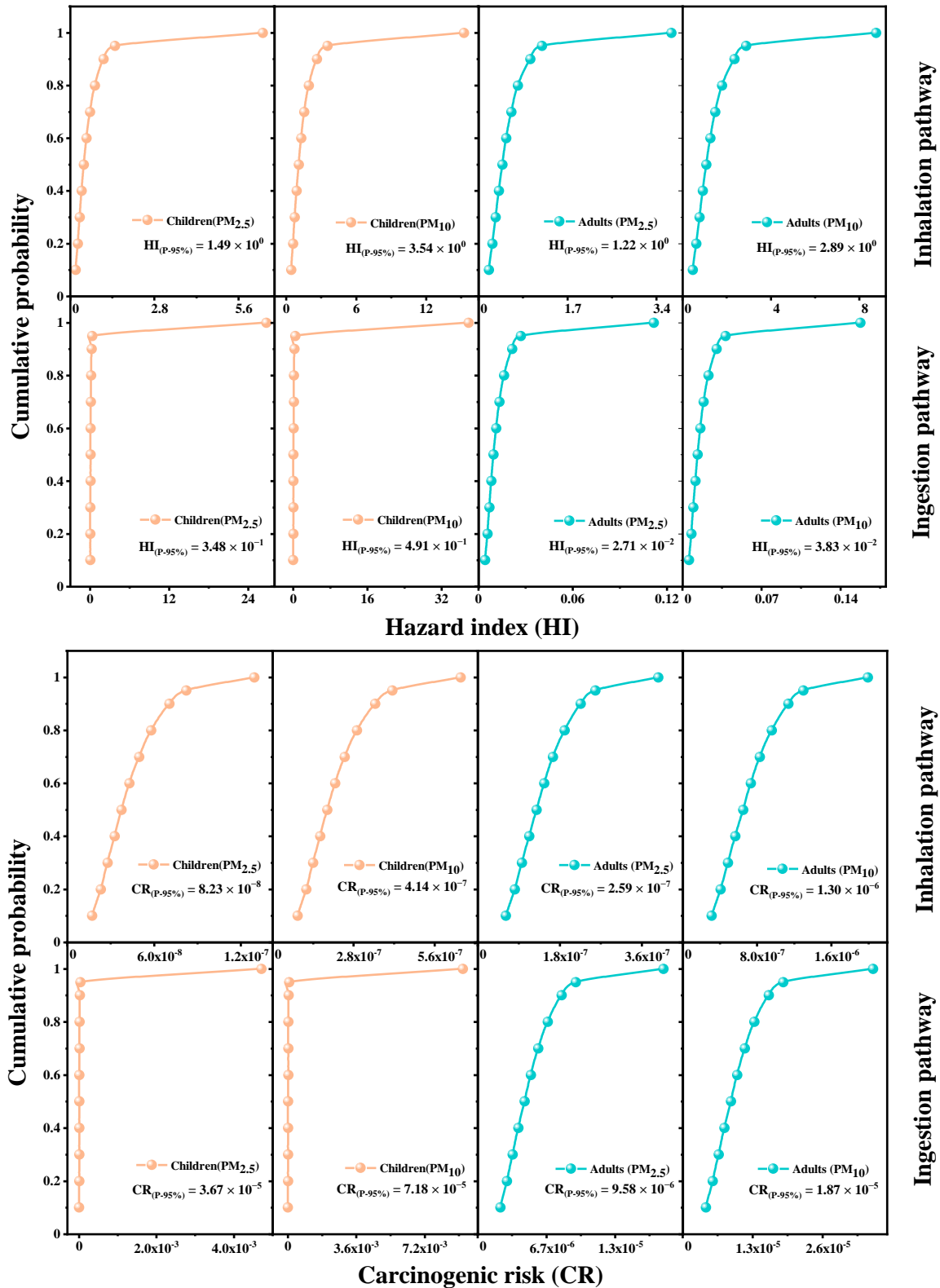


Figure 4. Cumulative probability distribution of carcinogenesis and non-carcinogenesis in summer.

4. Conclusions

The concentration of metals in PM₁₀ in the Hotan urban area had obvious temporal characteristics. The total average concentration of metals in summer is about 1.6 times that of winter, while the concentration in PM_{2.5} is not much different (about 1.06 times that of summer in winter), which is related to the impact of frequent sandstorms and dusty weather in local summer. Mn and Pb are the most abundant elements in each particle size segment in the Hotan area. The bioaccessibility of different kinds of heavy metals in simulated lung fluid and simulated gastrointestinal fluid differed greatly, with Cd having the highest bioaccessibility in the respiratory system in winter and Pb in summer. The solubility of Mn in gastric fluid was highest during the ingestion phase regardless of the season. Differences in the bioavailability of heavy metals were mainly related to the chemical composition of the simulated fluid and the form in which the metal was present in the particulate matter.

The results of the health risk assessment shown that, for non-carcinogenic risks, heavy metals pose a non-carcinogenic risk to both adults and children through the respiratory system in summer, but have almost no effect in winter; Mn was the main contributor to the risk value. However, Pb and Cd in winter pose a non-carcinogenic risk to children through ingestion. In terms of carcinogenic risk, there is no risk under the respiratory system, except for adults in winter, while there is a carcinogenic risk during the ingestion phase, regardless of season and population, and the risk is higher in children than in adults and in winter than in summer. As and Ni were the main contributors to the risk value. Monte Carlo simulations were used to calculate HI and CR values for the five metals in this study—with 10,000 iterations and a confidence level of 95%—and, compared with the USEPA standard model, the results showed that the trends in the conclusions were the same, and the risk values from the Monte Carlo simulations were slightly higher. In view of the above conclusions, Mn in wind and sand in arid regions can pose a risk to human health through respiration; Pb and Cd, mainly through the ingestion system, pose a non-carcinogenic risk to adults and children. In addition, the high concentrations of As and Ni in PM are the main reasons for the carcinogenic risk to the human body.

Supplementary Materials: The following supporting information can be downloaded at: <https://www.mdpi.com/article/10.3390/atmos14071066/s1>, Table S1: Detection limit of heavy metals ($\mu\text{g}/\text{mL}$); Table S2. Composition and pH of extraction fluids [62]; Table S3. Reference dose (RFD) and slope factors (SF) of different exposure pathway; Table S4. Parameter values used in ADD calculation models and Monte Carlo simulation of heavy metals in PM_{2.5} and PM₁₀ [63–65]; Table S5. Exposure concentration (EC_{inh}) ($\mu\text{g m}^{-3}$) and chemical daily intake (CDI_{ing}) ($\text{mg}\cdot\text{kg}^{-1}\cdot\text{d}^{-1}$) for each heavy metal by different pathways in winter; Table S6. Exposure concentration (EC_{inh}) ($\mu\text{g m}^{-3}$) and chemical daily intake (CDI_{ing}) ($\text{mg}\cdot\text{kg}^{-1}\cdot\text{d}^{-1}$) for each heavy metal by different pathways in summer; Table S7. The Pearson correlation coefficient matrix of heavy metals in PM_{2.5} and PM₁₀ of summer and winter; Table S8. Bioaccessibility of heavy metals in summer and winter; Table S9. Coefficient of variation for each metal in summer and winter.

Author Contributions: Conceptualization, B.L., D.T. and X.D.; methodology, B.L. and D.T.; software, B.L., Q.Z., X.Z. and R.Z.; validation, D.T., X.W., Q.Z., X.Z. and R.Z.; formal analysis, Y.Z.; investigation, Y.Z. and A.A.; resources, B.L. and Y.Z.; data curation, B.L.; writing—original draft preparation, B.L.; writing—review and editing, Y.Z.; visualization, Y.Z. and A.A.; supervision, D.T.; project administration, D.T. and X.D.; funding acquisition, D.T. and X.D.. All authors have read and agreed to the published version of the manuscript.

Funding: This research was funded by the National Natural Science Foundation of China (41967050/42177090).

Institutional Review Board Statement: Not applicable.

Informed Consent Statement: Not applicable.

Data Availability Statement: Data sharing is not applicable to this article.

Acknowledgments: Special thanks to Xiaoxiao Zhang for his guidance in the writing process.

Conflicts of Interest: The authors declare no conflict of interest.

References

1. Manisalidis, I.; Stavropoulou, E.; Stavropoulos, A.; Bezirtzoglou, E. Environmental and Health Impacts of Air Pollution: A Review. *Front. Public Health* **2020**, *8*, 14. [[CrossRef](#)] [[PubMed](#)]
2. Ali, M.U.; Liu, G.; Yousaf, B.; Ullah, H.; Abbas, Q.; Munir, M. A systematic review on global pollution status of particulate matter-associated potential toxic elements and health perspectives in urban environment. *Environ. Geochem. Health* **2019**, *41*, 1131–1162. [[CrossRef](#)] [[PubMed](#)]
3. He, F.; Shaffer, M.L.; Rodriguez-Colon, S.; Yanosky, J.D.; Bixler, E.; Cascio, W.E.; Liao, D. Acute Effects of Fine Particulate Air Pollution on Cardiac Arrhythmia: The APACR Study. *Environ. Health Perspect.* **2011**, *119*, 927–932. [[CrossRef](#)]
4. Kim, H.; Kim, H.; Park, Y.H.; Lee, J.T. Assessment of temporal variation for the risk of particulate matters on asthma hospitalization. *Environ. Res.* **2017**, *156*, 542. [[CrossRef](#)]
5. Hwang, B.F.; Lee, Y.L. Air Pollution and Prevalence of Bronchitic Symptoms Among Children in Taiwan. *Chest* **2010**, *138*, 956–964. [[CrossRef](#)]
6. Shang, Y.; Sun, Z.; Cao, J.; Wang, X.; Zhong, L. Systematic review of Chinese studies of short-term exposure to air pollution and daily mortality. *Environ. Int.* **2013**, *54*, 100–111. [[CrossRef](#)]
7. Wang, R.; Liu, J.; Qin, Y.; Chen, Z.; Li, J.; Guo, P.; Shan, L.; Li, Y.; Hao, Y.; Jiao, M.; et al. Global attributed burden of death for air pollution: Demographic decomposition and birth cohort effect. *Sci. Total Environ.* **2023**, *860*, 160444. [[CrossRef](#)]
8. Lee, K.S.; Min, W.K.; Choi, Y.J.; Jin, S.J.; Park, K.H.; Kim, S. The Effect of Maternal Exposure to Air Pollutants and Heavy Metals during Pregnancy on the Risk of Neurological Disorders Using the National Health Insurance Claims Data of South Korea. *Medicina* **2023**, *59*, 951. [[CrossRef](#)] [[PubMed](#)]
9. Okuda, T.; Katsuno, M.; Naoi, D.; Nakao, S.; Tanaka, S.; He, K.; Ma, Y.; Lei, Y.; Jia, Y. Trends in hazardous trace metal concentrations in aerosols collected in Beijing, China from 2001 to 2006. *Chemosphere* **2008**, *72*, 917–924. [[CrossRef](#)] [[PubMed](#)]
10. Galvao, E.S.; Santos, J.M.; Lima, A.T.; Reis, N.C.; Orlando, M.T.D.; Stuetz, R.M. Trends in analytical techniques applied to particulate matter characterization: A critical review of fundamentals and applications. *Chemosphere* **2018**, *199*, 546–568. [[CrossRef](#)]
11. Bollati, V.; Marinelli, B.; Apostoli, P.; Bonzini, M.; Nordio, F.; Hoxha, M.; Pegoraro, V.; Motta, V.; Tarantini, L.; Cantone, L. Exposure to metal-rich particulate matter modifies the expression of candidate microRNAs in peripheral blood leukocytes. *Environ. Health Perspect.* **2010**, *118*, 763–768. [[CrossRef](#)]
12. Wiseman, C.; Zereini, F. Characterizing metal(loid) solubility in airborne PM₁₀, PM_{2.5} and PM₁ in Frankfurt, Germany using simulated lung fluids. *Atmos. Environ.* **2014**, *89*, 282–289. [[CrossRef](#)]
13. Naujokas, M.F.; Anderson, B.; Ahsan, H.; Aposhian, H.V.; Graziano, J.H.; Thompson, C.; Suk, W.A. The Broad Scope of Health Effects from Chronic Arsenic Exposure: Update on a Worldwide Public Health Problem. *Environ. Health Perspect.* **2013**, *121*, 295–302. [[CrossRef](#)] [[PubMed](#)]
14. Fan, M.Y.; Zhang, Y.L.; Lin, Y.C.; Cao, F.; Fu, P. Specific sources of health risks induced by metallic elements in PM_{2.5} during the wintertime in Beijing, China. *Atmos. Environ.* **2020**, *246*, 118112. [[CrossRef](#)]
15. Dean, J.R.; Elom, N.I.; Entwistle, J.A. Use of simulated epithelial lung fluid in assessing the human health risk of Pb in urban street dust. *Sci. Total Environ.* **2017**, *579*, 387–395. [[CrossRef](#)] [[PubMed](#)]
16. Xin, H.; Zhang, Y.; Ding, Z.; Wang, T.; Lian, H.; Sun, Y.; Wu, J. Bioaccessibility and health risk of arsenic and heavy metals (Cd, Co, Cr, Cu, Ni, Pb, Zn and Mn) in TSP and PM_{2.5} in Nanjing, China. *Atmos. Environ.* **2012**, *57*, 146–152.
17. Behrooz, R.D.; Kaskaoutis, D.G.; Grivas, G.; Mihalopoulos, N. Human health risk assessment for toxic elements in the extreme ambient dust conditions observed in Sistan, Iran. *Chemosphere* **2020**, *262*, 127835. [[CrossRef](#)]
18. Sah, D.; Verma, P.K.; Kandikonda, M.K.; Lakhani, A. Pollution characteristics, human health risk through multiple exposure pathways, and source apportionment of heavy metals in PM₁₀ at Indo-Gangetic site. *Urban Clim.* **2019**, *27*, 149–162. [[CrossRef](#)]
19. Novo-Quiza, N.; Sanroman-Hermida, S.; Sanchez-Pinero, J.; Moreda-Pineiro, J.; Muniategui-Lorenzo, S.; Lopez-Mahia, P. In-vitro inhalation bioavailability estimation of Metal(oid)s in atmospheric particulate matter (PM_{2.5}) using simulated alveolar lysosomal fluid: A dialyzability approach. *Environ. Pollut.* **2023**, *317*, 8. [[CrossRef](#)]
20. Kasemodel, M.C.; Rodrigues, V.G.S. Soil Particle Size Fractioning and Pb and Cd Bioaccessibility on a Dirt Road Near Former Beneficiation and Smelting Plant. *Water Air Soil Pollut.* **2022**, *233*, 17. [[CrossRef](#)]
21. Huang, X.; Betha, R.; Tan, L.Y.; Balasubramanian, R. Risk assessment of bioaccessible trace elements in smoke haze aerosols versus urban aerosols using simulated lung fluids. *Atmos. Environ.* **2016**, *125*, 505–511. [[CrossRef](#)]
22. Morales, S.M.; Breton, J.G.C.; Carbajal, N.; Breton, R.M.C.; Severino, R.L.; Kahl, J.D.W.; Avila, J.R.C.; Lozada, S.E.C.; Guzman, A.E.; Pech, I.E.P.; et al. PM_{2.5}-bound trace metals in an urban area of Northern Mexico during the COVID-19 pandemic: Characterization, sources, and health risk. *Air Qual. Atmos. Health* **2023**.
23. Martin-Cruz, Y.; Gomez-Losada, A. Risk Assessment and Source Apportionment of Metals on Atmospheric Particulate Matter in a Suburban Background Area of Gran Canaria (Spain). *Int. J. Environ. Res. Public Health* **2023**, *20*, 5763. [[CrossRef](#)] [[PubMed](#)]
24. Poggio, L.; Vrscaj, B.; Schulin, R.; Hepperle, E.; Marsan, F.A. Metals pollution and human bioaccessibility of topsoils in Grugliasco (Italy). *Environ. Pollut.* **2009**, *157*, 680–689. [[CrossRef](#)]

25. Denys, S.; Caboche, J.; Tack, K.; Rychen, G.; Wragg, J.; Cave, M.; Jondreville, C.; Feidt, C. In Vivo Validation of the Unified BARGE Method to Assess the Bioaccessibility of Arsenic, Antimony, Cadmium, and Lead in Soils. *Environ. Sci. Technol.* **2012**, *46*, 6252. [[CrossRef](#)]
26. Smichowski, P.; Polla, G.; Gómez, D. Metal fractionation of atmospheric aerosols via sequential chemical extraction: A review. *Anal. Bioanal. Chem.* **2005**, *381*, 302–316. [[CrossRef](#)] [[PubMed](#)]
27. Mukhtar, A.; Limbeck, A. Recent developments in assessment of bio-accessible trace metal fractions in airborne particulate matter: A review. *Anal. Chim. Acta* **2013**, *774*, 11–25. [[CrossRef](#)]
28. Karthikeyan, S.; Joshi, U.M.; Balasubramanian, R. Microwave assisted sample preparation for determining water-soluble fraction of trace elements in urban airborne particulate matter: Evaluation of bioavailability. *Anal. Chim. Acta* **2006**, *576*, 23–30. [[CrossRef](#)]
29. Manousakas, M.; Papaefthymiou, H.; Eleftheriadis, K.; Katsanou, K. Determination of water-soluble and insoluble elements in PM_{2.5} by ICP-MS. *Sci. Total Environ.* **2014**, *493*, 694–700. [[CrossRef](#)]
30. Davison, W.; Arewgoda, C.M.; Hamilton-Taylor, J.; Hewitt, C.N. Kinetics of dissolution of lead and zinc from rural atmospheric aerosols in freshwater and synthetic solutions. *Water Res.* **1994**, *28*, 1703–1709. [[CrossRef](#)]
31. Hamilton-Taylor, J.; Yang, Y.L.; Arewgoda, C.M.; Hewitt, C.N.; Davison, W. Trace metal dissolution kinetics of three rural atmospheric aerosols in a range of natural fresh water types. *Water Res.* **1993**, *27*, 243–254. [[CrossRef](#)]
32. Wiseman, C.L.S.; Niu, J.; Levesque, C.; Chenier, M.; Rasmussen, P.E. An assessment of the inhalation bioaccessibility of platinum group elements in road dust using a simulated lung fluid. *Environ. Pollut.* **2018**, *241*, 1009–1017. [[CrossRef](#)]
33. Luo, X.S.; Yu, S.; Li, X.D. Distribution, availability, and sources of trace metals in different particle size fractions of urban soils in Hong Kong: Implications for assessing the risk to human health. *Environ. Pollut.* **2011**, *159*, 1317–1326. [[CrossRef](#)] [[PubMed](#)]
34. Bi, X.; Li, Z.; Sun, G.; Liu, J.; Han, Z. In vitro bioaccessibility of lead in surface dust and implications for human exposure: A comparative study between industrial area and urban district. *J. Hazard. Mater.* **2015**, *297*, 191–197. [[CrossRef](#)]
35. Wragg, J.; Cave, M.; Basta, N.; Brandon, E.; Casteel, S.; Denys, S.; Gron, C.; Oomen, A.; Reimer, K.; Tack, K. An inter-laboratory trial of the unified BARGE bioaccessibility method for arsenic, cadmium and lead in soil. *Sci. Total Environ.* **2011**, *409*, 4016–4030. [[CrossRef](#)] [[PubMed](#)]
36. Liu, K.; Ren, J. Characteristics, sources and health risks of PM_{2.5}-bound potentially toxic elements in the northern rural China. *Atmos. Pollut. Res.* **2019**, *10*, 1621–1626. [[CrossRef](#)]
37. Huang, R.-J.; Cheng, R.; Jing, M.; Yang, L.; Li, Y.; Chen, Q.; Chen, Y.; Yan, J.; Lin, C.; Wu, Y.; et al. Source-specific health risk analysis on particulate trace elements: Coal combustion and traffic emission as major contributors in wintertime Beijing. *Environ. Sci. Technol.* **2018**, *52*, 10967–10974. [[CrossRef](#)] [[PubMed](#)]
38. Yang, X.; Eziz, M.; Hayrat, A.; Ma, X.; Yan, W.; Qian, K.; Li, J.; Liu, Y.; Wang, Y. Heavy Metal Pollution and Risk Assessment of Surface Dust in the Arid NW China. *Int. J. Environ. Res. Public Health* **2022**, *19*, 13296. [[CrossRef](#)]
39. Bao, Y.; Xie, H.; Zhang, Y.; Zhang, K.; Yang, H.; Chen, T. PM_{2.5} and PM₁₀ Pollution Characteristics during Summer in Hotan City and Relevant Health Risk Assessment. *Environ. Sci. Technol.* **2022**, *45*, 154–162.
40. Zoitos, B.K.; Meringo, A.D.; Rouyer, E.; Bauer, S.T.J.; Law, B.; Boymel, P.M.; Olson, J.R.; Christensen, V.R.; Guldborg, M.; Koenig, A.R.; et al. In vitro measurement of fiber dissolution rate relevant to biopersistence at neutral pH: An interlaboratory round robin. *Inhal. Toxicol.* **1997**, *9*, 525–540.
41. Ruby, M.V.; Davis, A.; Schoof, R.; Eberle, S.; Sellstone, C.M. Estimation of Lead and Arsenic Bioavailability Using a Physiologically Based Extraction Test. *Environ. Sci. Technol.* **1996**, *30*, 422–430. [[CrossRef](#)]
42. Zia, M.H.; Codling, E.E.; Scheckel, K.G.; Chaney, R.L. In vitro and in vivo approaches for the measurement of oral bioavailability of lead (Pb) in contaminated soils: A review. *Environ. Pollut.* **2011**, *159*, 2320–2327. [[CrossRef](#)] [[PubMed](#)]
43. Deshommès, E.; Tardif, R.; Edwards, M.; Sauvé, S.; Prévost, M. Experimental determination of the oral bioavailability and bioaccessibility of lead particles. *Chem. Cent. J.* **2012**, *6*, 1–31. [[CrossRef](#)] [[PubMed](#)]
44. USEPA. *Risk Assessment Guidance for Superfund Volume I Human Health Evaluation Manual. (Part A); (Part F: Supplemental Guidance for Inhalation Risk Assessment)*; Environmental Protection Agency: Washington, DC, USA, 2011.
45. Turap, Y.; Talifu, D.; Wang, X.; Ding, X.; Abulizi, A.; Maihemuti, M.; Yiming, M. Elemental Characterization in PM_{2.5} during the Dust and Non-dust Periods in the Extremely-arid Areas. *Ecol. Environ. Sci.* **2017**, *26*, 1529.
46. An, J.; Liu, H.; Wang, X.; Talifu, D.; Abulizi, A.; Maihemuti, M.; Li, K.; Bai, H.; Luo, P.; Xie, X. Oxidative potential of size-segregated particulate matter in the dust-storm impacted Hotan, northwest China. *Atmos. Environ.* **2022**, *280*, 119142. [[CrossRef](#)]
47. Liu, H.; Wang, X.; Talifu, D.; Ding, X.; Abulizi, A.; Tursun, Y.; An, J.; Li, K.; Luo, P.; Xie, X. Distribution and sources of PM_{2.5}-bound free silica in the atmosphere of hyper-arid regions in Hotan, North-West China. *Sci. Total Environ.* **2022**, *810*, 152368. [[CrossRef](#)]
48. Gao, P.; Guo, H.; Zhang, Z.; Ou, C.; Hang, J.; Fan, Q.; He, C.; Wu, B.; Feng, Y.; Xing, B. Bioaccessibility and exposure assessment of trace metals from urban airborne particulate matter (PM₁₀ and PM_{2.5}) in simulated digestive fluid. *Environ. Pollut.* **2018**, *242*, 1669–1677. [[CrossRef](#)]
49. Sun, Y.; Hu, X.; Wu, J.; Lian, H.; Chen, Y. Fractionation and health risks of atmospheric particle-bound As and heavy metals in summer and winter. *Sci. Total Environ.* **2014**, *493*, 487–494. [[CrossRef](#)]
50. Mbengue, S.; Alleman, L.Y.; Flament, P. Bioaccessibility of trace elements in fine and ultrafine atmospheric particles in an industrial environment. *Environ. Geochem. Health* **2015**, *37*, 875–889. [[CrossRef](#)]
51. Hamad, S.H.; Schauer, J.J.; Shafer, M.M.; Al-Rheem, E.A.; Skaar, P.S.; Heo, J.; Tejedor-Tejedor, I. Risk assessment of total and bioavailable potentially toxic elements (PTEs) in urban soils of Baghdad-Iraq. *Sci. Total Environ.* **2014**, *494*, 39–48. [[CrossRef](#)]

52. Lin, Y.C.; Zhang, Y.L.; Song, W.; Yang, X.; Fan, M.Y. Specific sources of health risks caused by size-resolved PM-bound metals in a typical coal-burning city of northern China plain during the winter haze event. *Sci. Total Environ.* **2020**, *734*, 138651. [[CrossRef](#)] [[PubMed](#)]
53. Pan, Y.; Tian, S.; Li, X.; Sun, Y.; Li, Y.; Wentworth, G.R.; Wang, Y. Trace elements in particulate matter from metropolitan regions of Northern China: Sources, concentrations and size distributions. *Sci. Total Environ.* **2015**, *537*, 9–22. [[CrossRef](#)]
54. Liang, B.; Li, X.-l.; Ma, K.; Liang, S.-X. Pollution characteristics of metal pollutants in PM_{2.5} and comparison of risk on human health in heating and non-heating seasons in Baoding, China. *Ecotoxicol. Environ. Saf.* **2018**, *170*, 166–171. [[CrossRef](#)] [[PubMed](#)]
55. Mayer, R.A.; Godwin, H.A. Preparation of media and buffers with soluble lead. *Anal. Biochem.* **2006**, *356*, 142–144. [[CrossRef](#)]
56. Barsby, A.; McKinley, J.M.; Ofterdinger, U.; Young, M.; Cave, M.R.; Wragg, J. Bioaccessibility of trace elements in soils in Northern Ireland. *Sci. Total Environ.* **2012**, *433*, 398–417. [[CrossRef](#)]
57. Rodrigues, S.M.; Henriques, B.; Silva, E.F.D.; Pereira, M.E.; Duarte, A.C.; Roemkens, P.F.A.M. Evaluation of an approach for the characterization of reactive and available pools of twenty potentially toxic elements in soils: Part I—The role of key soil properties in the variation of contaminants' reactivity. *Chemosphere* **2010**, *81*, 1549–1559. [[CrossRef](#)]
58. Qu, C.; Li, B.; Wu, H.; Wang, S.; Giesy, J.P. Multi-pathway assessment of human health risk posed by polycyclic aromatic hydrocarbons. *Environ. Geochem. Health* **2015**, *37*, 587–601. [[CrossRef](#)]
59. Othman, M.; Latif, M.T.; Mohamed, A.F. Health impact assessment from building life cycles and trace metals in coarse particulate matter in urban office environments. *Ecotoxicol. Environ. Saf.* **2018**, *148*, 293–302. [[CrossRef](#)]
60. Chiang, K.C.; Chio, C.P.; Chiang, Y.H.; Liao, C.M. Assessing hazardous risks of human exposure to temple airborne polycyclic aromatic hydrocarbons. *J. Hazard. Mater.* **2009**, *166*, 676–685. [[CrossRef](#)]
61. Nie, D.; Wu, Y.; Chen, M.; Liu, H.; Zhang, K.; Ge, P.; Yuan, Y.; Ge, X. Bioaccessibility and health risk of trace elements in fine particulate matter in different simulated body fluids. *Atmos. Environ.* **2018**, *186*, 1–8. [[CrossRef](#)]
62. Huang, H.; Ying, J.; Xu, X.; Cao, X. In vitro bioaccessibility and health risk assessment of heavy metals in atmospheric particulate matters from three different functional areas of Shanghai, China. *Sci. Total Environ.* **2018**, *610*, 546–554. [[CrossRef](#)] [[PubMed](#)]
63. USEPA. *Supplemental Guidance for Developing Soil Screening Levels for Superfund Sites*; Environmental Protection Agency: Washington, DC, USA, 2002.
64. Duan, X.L. *Exposure Factors Handbook of Chinese Population*; China Environment Science Press: Beijing China, **2013**.
65. USEPA. *Risk Assessment Guidance for Superfund, Volume I: Human Health Evaluation Manual (Part E, Supplemental Guidance for Dermal Risk Assessment)*; Environmental Protection Agency: Washington, DC, USA, 2001.

Disclaimer/Publisher's Note: The statements, opinions and data contained in all publications are solely those of the individual author(s) and contributor(s) and not of MDPI and/or the editor(s). MDPI and/or the editor(s) disclaim responsibility for any injury to people or property resulting from any ideas, methods, instructions or products referred to in the content.